
**BIOPHYSICS
AND MEDICAL PHYSICS**

Computed Tomography Scan Optimization of Chest and Abdomen Protocols

M'hamed El Mansouri^{a,*}, Abdelmajid Choukri^a, Mohammed Talbi^b, and Hajar Khallouki^c

^a *Ibn Tofail University, Faculty of Sciences, Department of Physics, Laboratory of Materials and Subatomic Physics P.O. Box 133, Kenitra, Morocco*

^b *Moulay Ismail University, Faculty of Sciences, Physical Sciences and Engineering, ENPT P.O. Box 11201, Zitoune Meknes, Morocco*

^c *Hassan 1st University, Faculty of Sciences and Techniques P.O. Box 577, Settat, Morocco*

**e-mail: m.elmansouri@uhp.ac.ma*

Received December 25, 2021; revised February 2, 2022; accepted February 2, 2022

Abstract—This work aims to optimize the scanning parameters of Chest and Abdomen protocols in computed tomography, whilst maintaining image quality and reducing the dose. Two phantoms have been used to evaluate the dose and image quality on a 16-slice HITACHI CT system by establishing the optimization threshold for each protocol. The proposed Thoracic protocol has shown a reduction in Computed Tomography Dose Index (CTDIvol) and Contrast-Noise Ratio (CNR), and the spatial resolution has remained stable with a slight increase in noise. For the optimized Abdominal protocol, CTDIvol has reduced significantly, noise has increased at the two new proposed energies of 100 and 120 kV, and CNR has decreased. This research has shown that by optimizing Chest and Abdomen protocols, substantial dose reductions may be achieved without compromising image quality when using a multi-slice Scanner.

Keywords: CT scan, CTDI, image quality, phantom, protocol

DOI: 10.3103/S0027134922010155

INTRODUCTION

Morocco has developed an important medical imaging infrastructure; this development is reflected in the increase in the number of medical equipment, with more than 424 radiology departments and centers. This number is expected to increase in the future to reach more than 360 scanners [1]. Computed tomography (CT) scans provide higher doses than other imaging procedures, and can potentially promote risks [2]. Thus, several studies have been carried out to assess the risks of CT scans [3–5], and to seek the protocols' optimization [6, 7]. These studies have shown that exposure to ionizing radiation during CT examinations, can be associated with an increase in the appearance of long-term genetic mutations and radiation-induced cancers, through stochastic effects [8]. A single CT scan subjects the human body to 150–1100 times more radiation than a conventional X-ray scan, or about one year of exposure to radiation from natural and artificial sources in the environment [9, 10]. Clinically, the majority of radiology centers use protocols that are preprogrammed on devices. Consequently, they are not always suitable for clinical cases (pediatrics, patients' corpulence) [10]. It is essential to justify and ensure quality examinations with the lowest possible dose. These conditions

depend on the parameters' choice. A successful CT scan diagnosis requires high-quality images with an optimal patient dose. The compromise between image quality and dosimetry in CT scans is the subject of numerous radiation protection reports and scientific publications [11, 12].

The quality of the image provided by CT scanners can be assessed by the objective measurement of physical quantities such as CT number, low contrast detectability, noise, linearity, spatial resolution, and uniformity. These physical quantities can be measured by several phantoms such as the American College of Radiology (ACR phantom) [13], Catphan 500 [14], and other types. These different phantoms are used as a reference in the acceptance of quality assurance [15]. The calculation of the received doses by patients during a CT procedure is very complex [16], hence the need to use dosimetric quantities; such as the CT dose index (CTDI) which indicates the dose transferred to standard phantoms (16 cm for the skull and 32 cm for the body), and dose length product (DLP) which is defined as the volumetric (CTDIvol) multiplied by the length [17].

Although Morocco has a very large number of scanner units, no quality assurance system has been set up as recommended by the International Atomic

Energy Agency (IAEA) and the International Commission on Radiological Protection (ICRP) [15, 18]. Moreover, the limitations of the previous research in this context in Morocco prompted us to carry out this study. We aim to optimize the practices by evaluating the impact of acquisition parameters in computed tomography, which act effectively on the quality of image and dose [18, 19].

The volumetric computed tomography dose index $CTDI_{vol}$ was estimated using a polymethylmethacrylate (PMMA) phantom and a pencil ionization chamber [8]. In addition, the image quality variables including image noise, spatial resolution (SR), and noise-to-contrast ratio (CNR) were evaluated using a Catphan 500.

This study aims to optimize the practices of the chest and abdomen protocols in CT scan in Morocco, by showing that changing the acquisition parameters; (KVp and mAs) can reduce the dose (CTDI) while maintaining an image of optimal quality (noise, SR, and CNR). Therefore, we have varied the acquisition parameters to obtain images that provide the maximum amount of information to make a reliable diagnosis.

1. MATERIALS AND METHODS

Before starting the measurements, we performed the warmup and the air calibration on a HITACHI Supria 16-slice, installed in a Moroccan Hospital since 2015, with a workload of 20 patients per day. According to a questionnaire carried out at this hospital, we focused in this study only on two examination protocols, representing almost half of all the requested examinations (chest and abdomen). In addition, we have collected the 4 most frequent acquisition parameters by protocol. These same collected parameters are scanned through two phantoms evaluating the dose and the image quality while recording the values of the measured quantities ($CTDI_{vol}$, spatial resolution, contrast to noise ratio CNR, and noise).

Furthermore, these phantoms were re-scanned trying to find the threshold of optimal optimization, by reducing the parameters (KV and mAs) for the two protocols; chest and abdomen, until the quantities of the images' quality were considerably low. We deactivated the automatic dose modulation system and we performed two series of measurements using the two phantoms; in the first series of the chest protocol we reduced the kVp and increased the mAs, and in the second series of the abdomen protocol we reduced the mAs while switching between reductions, with no change in kVp.

Regarding the objective evaluation of the physical quantities of image quality in CT, we used a Catphan 500 phantom (Phantom Laboratory, Salem NY, USA). It consists of 4 modules enclosed in a box of 20 cm in diameter as shown in (Fig 1). The image



Fig. 1. Catphan 500.

quality quantities which were evaluated in this study are the spatial resolution (module CTP528), CNR (module CTP515), and noise (module CTP486) [20].

The first measured quantity was the image noise. It is obtained by calculating the standard deviation in a circular ROI which covers 40 of the homogeneous module diameter of a Catphan phantom, by plotting 5 ROI on the console image obtained after the scans; one in the center and 4 at the periphery (0° , 90° , 180° , and 270°) [21], using the following Eq. (1):

$$B = \frac{\sigma}{NS_{eau} - NS_{air}} \times 100\%, \quad (1)$$

where B is noise, σ is the standard deviation, NS_{eau} is the CT of water, and NS_{air} is the CT of air.

The second measured quantity was the CNR contrast-to-noise ratio using the CTP515 module's image, as shown in Eq. (2):

$$CNR = \frac{\text{number}CT_{int} - \text{number}CT_{ext}}{SD}, \quad (2)$$

where CT_{int} is the CT number inside the circle, CT_{ext} is the CT number outside the circle, and SD (standard deviation). Contrast to noise ratio (CNR) is calculated for the 15 mm circle, with a contrast diameter of the CTP515 module's image [21]. Also, the number CT is defined by Eq. (3):

$$N_{CT} = \frac{\mu_{tissue} - \mu_{eau}}{\mu_{eau}} \times 1000, \quad (3)$$

where μ_{tissue} is the attenuation coefficient of tissue, and μ_{eau} is the attenuation coefficient of water.

The last measured quantity was the spatial resolution, by counting the number of line pairs per centimeter [22].

As for the dose measurement, the same variations in the scan parameters are applied using a cylindrical phantom with a diameter of 32 cm, simulating the adult body in (Fig 2). This phantom is of type PMMA

(Polymethyl-Methacrylate), of (1.19 g/cm³) density, and contains 5 holes (center, 3 h, 6 h, 9 h, and 12 h) [23]. We also used a calibrated pencil ionization chamber (model 10X6-3CT) [24], with an active length of 100 mm, measurement accuracy of ± 4 a dose measurement range of (200 nGy–1 kGy), an electrometer of type (RADCAL CORPORATION, California, USA), and Accu-Gold+ interface software for displaying the output parameters. First, we measured the CTDI₁₀₀ using the pencil ionization chamber [20], and then we calculated the CTDI_w based on the following Eq. (4):

$$CTDI_w = 1/3CTDI_{(100,c)} + 2/3CTDI_{(100,p)} \text{ (mGy)}, \quad (4)$$

where $CTDI_w$ is the weighted computed tomography dose index; $CTDI_{(100,c)}$ at the center, and $CTDI_{(100,p)}$ at the periphery. The $CTDI_{vol}$ was calculated by dividing the $CTDI_w$ by the factor of the pitch (1.06).

2. RESULTS

Three physical quantities of the image's quality including noise, spatial resolution, and contrast to noise ratio, as well as the CTDI of the two CT examinations were evaluated to identify the threshold of optimization, in order to determine new scanning protocols. Table 1 shows the chest examination results and Table 2 shows the abdomen examination results. For the thoracic protocol, the noise was the first quantity of image quality which was evaluated in Table 1. From 120 to 100 kV, the average values are increased from 11.82% to 38.17%. The measured average noise was high for the low currents of the mAs tube, and its behavior was downward by increasing the mAs, which matches the results of low contrast.

The second evaluated quantity was the spatial resolution. Using the CTP528 module from Catphan, we noted the average values as a function of the variation in kVp and mAs. For the old parameters, the values vary between 6 and 7 pl/cm with energies 120 kV; 6 at mAs between (75–90), and 7 pl/cm at mAs (115–165).



Fig. 2. PMMA.

The same values for the new parameters of 100 kV; 6 pl/cm at mAs between (115 and 143), and 7 pl/cm at mAs between (176 and 230).

Also, for the chest protocol, the CNR was the third evaluated quantity of the 15 mm circle's diameter at a 1% contrast, from the CTP515 module's image (Table 1). We have noticed that the values of CNR as a function of the 120 kV energy of the old parameters increase with the increase in mAs, going from 0.76 to 1.56. In addition, the rate of change between the new and old parameters fell slightly from 11.53% to 17.10% for the abdomen protocol, we proposed two new energies 100 kV and 120 kV for the noise quantity; noise at 100 kV increases from 48.08% to 52.55% with the increase in mAs. On the other hand, at 120 kV the noise increases slightly from 24.41% to 25.55% with the decrease in mAs. Regarding the spatial resolution, the values increase considerably with the tube energies; 6 pl/cm at 100KV with mAs: 200–210, and 7 pl/cm at 120 kV with mAs: 130–300. The old values of the spatial resolution were higher compared to the new values especially in low energy (100 kVp).

Towards the CNR of the abdomen protocol, the variations in the mean values experienced a slight increase with the increase in mAs. The variation rates,

Table 1. Current and new scanning protocols for Chest

Old scan	kV mAs	CTDIvol	NOISE	SR	CNR
	120 75	5.82	8.20	6	0.76
	120 90	6.75	7.61	6	1.13
	120 115	8.96	6.60	7	1.33
	120 165	10.70	5.15	7	1.56
New scan	kV mAs	CTDIvol	NOISE	SR	CNR
	100 115	4.87	9.35	6	0.63
	100 143	5.76	8.51	6	0.99
	100 176	6.28	7.94	7	1.15
	100 230	7.95	6.91	7	1.38

Table 2. Current and new scanning protocols for Abdomen

Old scan	kV mAs	CTDIvol	NOISE	SR	CNR
	120 155	10.56	5.36	7	1.41
	120 210	11.72	4.48	7	1.63
	120 265	14.52	4.11	7	1.79
	120 300	15.85	3.85	7	1.96
New scan	kV mAs	CTDIvol	NOISE	SR	CNR
	120 130	9.81	6.73	7	1.15
	100 210	7.26	6.66	6	1.40
	100 200	7.55	6.27	6	1.52
	120 240	11.60	4.79	7	1.55

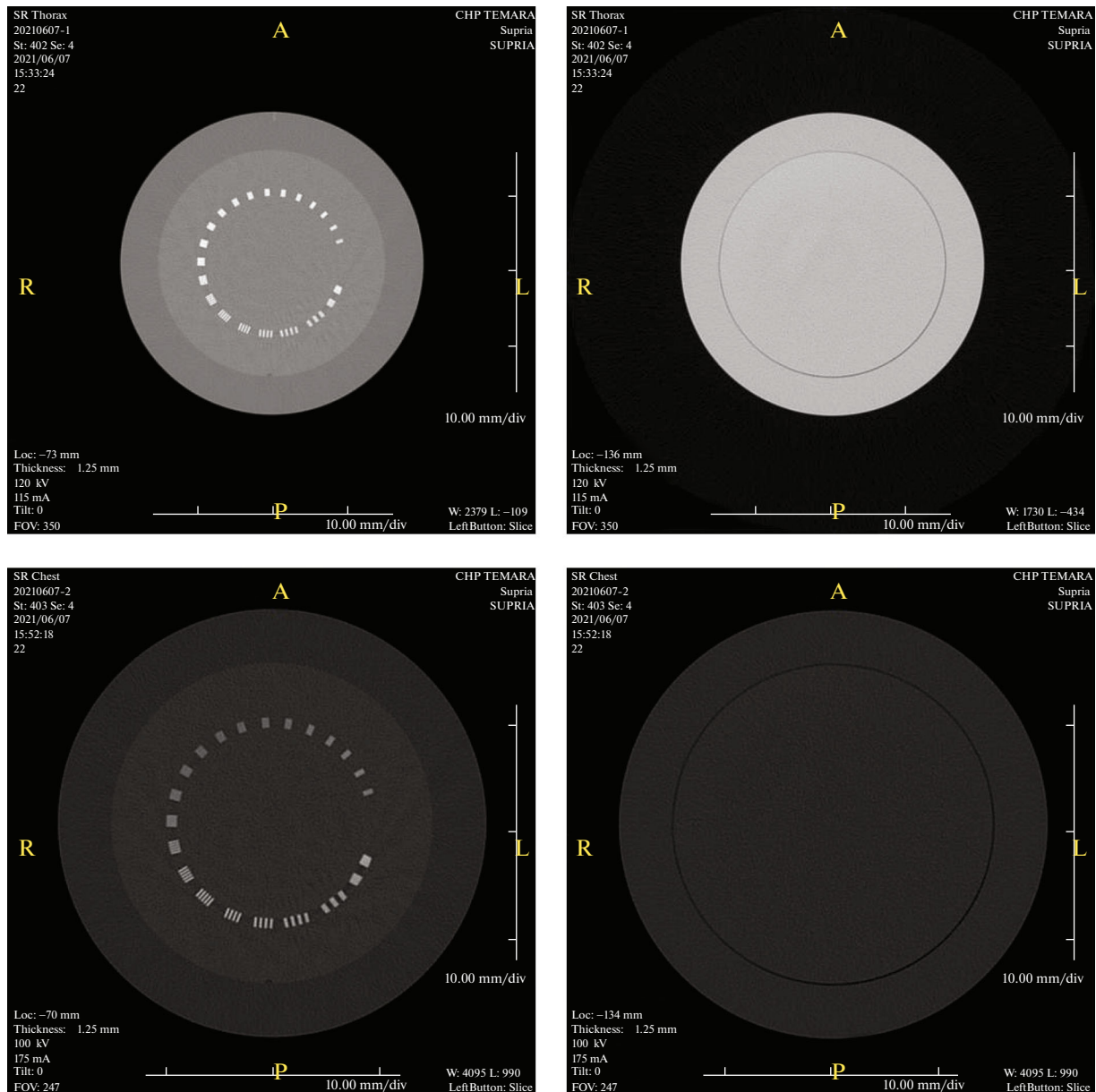


Fig. 3. (a) SR of 120 kV|115 mAs for Chest. (b) Image Noise of 120 kV|115 mAs for Chest, (c) SR of 100 kV|176 mAs for Chest, (d) Image Noise of 100 kV|176 mAs for Chest.

between the old parameters and the new parameters, vary between 14.11% and 20.21%. The $CTDI_{vol}$ of the two protocols is presented in Tables 1 and 2. For the chest examination, the $CTDI_{vol}$ obtained at 120 kV varies between 5.82 and 10.70 mGy, and the $CTDI_{vol}$ obtained at 100 kV varies between 4.84 and 7.85 mGy. In addition, the rate of change from 120 kV to 100 kV was reduced from 14.66% to 39.70%.

Compared to the abdomen examination, the rate of change of the $CTDI_{vol}$ was from 7.10% to 48%, when

switching from the old parameters to the new ones. In this study, we used the $CTDI_{vol}$ measurement, which is a good CT index used to estimate the radiation dose to patients. This index is a good indicator of comparison between the different acquisition parameters which are already studied. Our work has shown that reducing the radiation dose to patients is possible by changing the acquisition parameters of the two protocols used by the HITACHI scanner.

The two (Figs. 3a and 3b), represent the measured quantities of spatial resolution and noise at (120 kV

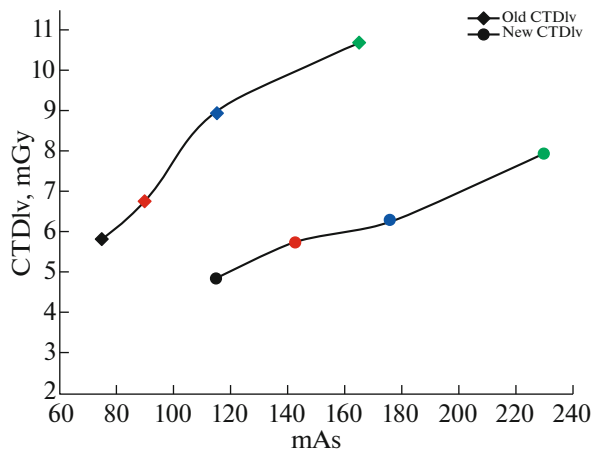


Fig. 4. Current and new CTDIvol for Chest.

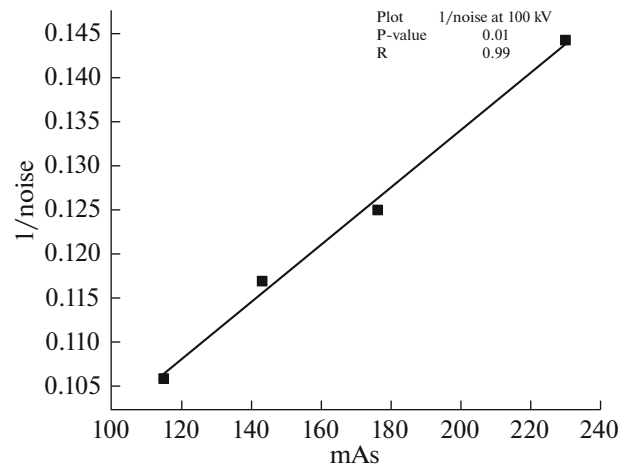


Fig. 5. Correlation between noise and mAs for Chest.

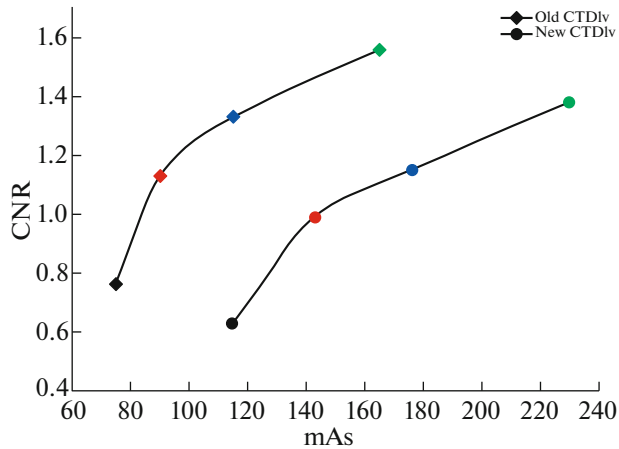


Fig. 6. Current and new CNR for Chest.

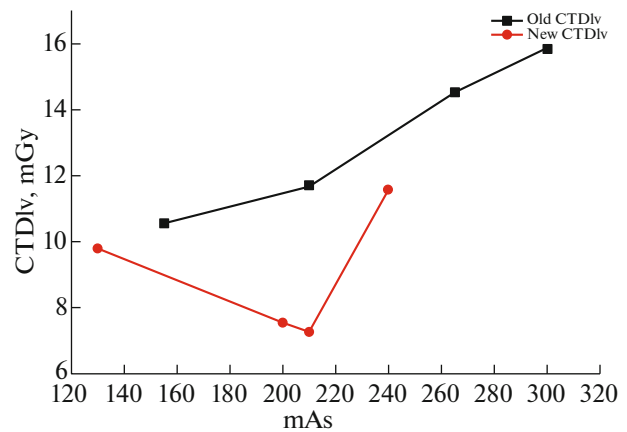


Fig. 7. Current and new CTDIvol for Abdomen.

and 115 mAs) for the thoracic protocol. However, the two (Figs. 3c and 3d), are for the new thoracic protocol proposed at (100 kV and 175 mAs).

3. DISCUSSION

16 different scans were performed for two anatomical regions (chest and abdomen), divided into two series; one for the current protocol, and the other for the proposed protocol while taking into account the image quality degradation. For both exams, the automatic tube current modulation option was deactivated during the Catphan 500 scan and the mAs were set manually, as there would have been no change in mAs given that there is no variation in the scanned phantom (the diameter of the Catphan 500 phantom is invariable). The obtained results are plotted on the following graphs to fully understand the behavior of the physical magnitudes of the image, and the dose as a function of the variation in the acquisition parameters.

Regarding the thoracic examination, the reduction in kV by 16.66%, accompanied by an increase in mAs from mAs from 39% to 58%, made it possible to reduce the CTDI from 14.66% to 39.70% (Fig 4), with an increase in noise of 11.82 at 38%, this matches with the conclusions found by Francis Zarb et al. [25]. Authors in [25] reduced kV from 14% to 17%, which allowed a dose reduction from 32% to 38%, with a considerable increase in noise from 16% to 29%, this noise was inversely correlated with mAs (Fig 5). By switching from the current protocol to the proposed one, the CNR was reduced from 11.54% to 17.10% (Fig. 6), and the spatial resolution was not affected. This is consistent with the previous studies done by Kun Tang et al. [26].

Regarding the abdomen examination, we opted for two changes; the first one was the reduction in mAs, and the second one was the combination of the two parameters (mAs and kV). The reductions in mAs from 16.12% to 20% made it possible to reduce the

dose from 7.10% to 26.01% (Fig. 7), with an increase in noise from 24.41% to 25.55%, and a reduction in CNR from 18.43% to 20.21%. This is consistent with the results of Francis Zarb et al. [25] who have shown that the reduction of mAs from 20% to 33% makes it possible to reduce the CTDI in the same way from 20% to 33%, with an increase in noise from 3% to 27%. Regarding the reduction of kV by 16.66%, the CTDI was reduced from 38.05% to 48.00%, the noise increased from 11.82% to 38.17%, and the CNR was lowered from 12.38% to 13.53%. The SR was reduced from 7 to 6 pl/cm, which is consistent with the studies of Zaehringer et al. [27], and Martin Beeres et al. [28] who concluded that lowering kV reduces the dose without compromising the image quality.

Changing the tube currents (mAs), slice thickness, collimation, the field of view, vary the values of the Hounsfield units slightly. Also changing the tube voltage (kVp) and changing the reconstruction filters have a very large impact on the HU units. To understand how changing the acquisition parameters affects the HU units and their impact on the dose change, it is recommended to use a phantom containing inserts that simulate the human body, such as the CIRS phantom.

CONCLUSIONS

Several studies have cited reliable methods for achieving low dose and adequate image quality in CT scanning with optimized practices, including a correct selection of tube current and voltage according to patient body size and other criteria. Reaching this goal requires a considerable knowledge base in radiation protection and hence the need to keep the dose as low as possible. This research has shown that by optimizing chest and abdomen protocols, substantial dose reductions may be achieved without compromising image quality and with no degradation of spatial resolution.

REFERENCES

1. H. Saikouk, I. Ou-Saada, F. Bentayeb, S. Boutayeb, and K. Eddaoui, "Medical physics status in Morocco: Education, training, and evolution," *Med. Phys. Int.* **7**, 282 (2019).
2. M. Alkhorayef, A. Sulieman, B. Alonazi, M. Alnaaimi, M. Alduaij, and D. Bradley, *Radiat. Phys. Chem.* **155**, 65–68 (2019).
<https://doi.org/10.1016/j.radphyschem.2018.08.019>
3. F. Caro, P. Smeets, L. Lapeire, E. Achten, and K. Bacher, *Phys. Med.* **52** (8), 32 (2018).
<https://doi.org/10.1016/j.ejmp.2018.06.153>
4. S. Semghouli, B. Amaoui, A. El Kharras, K. Bouykh-laf, O. K. Hakam, and A. Choukri, *Perspect Sci.* **12**, 100407 (2019).
<https://doi.org/10.1016/j.pisc.2019.100407>
5. S. Semghouli, B. Amaoui, A. Kharras, A. Shaim, O. Hakam, and A. Choukri, *Br. J. Appl. Sci. Technol.* **20** (3), 1–8 (2017).
<https://doi.org/10.9734/bjast/2017/32491>
6. K. Martini, J. W. Moon, M. P. Revel, S. Dangeard, C. Ruan, and G. Chassagnon, *Diagn. Interv. Imaging* **101**, 269–279 (2020).
<https://doi.org/10.1016/j.diii.2020.01.012>
7. M. El Mansouri, M. Talbi, A. Choukri, O. Nhila, and M. Aabid, *Radioprotection* (2022, in press).
<https://doi.org/10.1051/radiopro/2021035>
8. AAPM Reports - The Measurement, Reporting, and Management of Radiation Dose in CT. <https://www.aapm.org/pubs/reports/detail.asp?docid=97>. Accessed March 5, 2020.
9. M. ElMansouri, A. Choukri, M. Talbi, and O. K. Hakam, *Atom Indones.* **47**, 105–109 (2021).
<https://doi.org/10.17146/aij.2021.1120>
10. M. Rawashdeh, M. F. McEntee, M. Zaitoun, et al., *Jordan. Comput. Biol. Med.* **102**, 132–137 (2018).
<https://doi.org/10.1016/j.compbiomed.2018.09.020>
11. D. Khoramian, S. Sistani, and R. A. Firouzjiah, *Polish J. Radiol.* **84**, e61–e67 (2019).
<https://doi.org/10.5114/pjr.2019.82743>
12. J. B. Moser, S. L. Sheard, S. Edyvean, and I. Vlahos, *Clin. Radiol.* **72**, 407–420 (2017).
<https://doi.org/10.1016/j.crad.2016.11.021>
13. B. Alikhani, L. Jamali, H. J. Raatschen, F. Wacker, and T. Werncke, *Radiography.* **23**, 202–210 (2017).
<https://doi.org/10.1016/j.radi.2017.03.013>
14. Catphan 500-600 Manual. <https://www.uio.no/studier/emner/matnat/fys/nedlagte-emner/FYS4760/h07/Catphan500-600manual.pdf>. Accessed March 5, 2020.
15. K. Gulliksrud, C. Stokke, and A. C. Martinsen, *Phys. Med.* **30**, 521–526 (2014).
<https://doi.org/10.1016/j.ejmp.2014.01.006>
16. B. Newman, A. Ganguly, J. E. Kim, and T. Robinson, *Am. J. Roentgenol.* **199** (2) (2012).
<https://doi.org/10.2214/AJR.10.5895>
17. B. Habib Geryes, A. Hornbeck, V. Jarrige, N. Pierrat, H. Ducou le Pointe, and S. Dreuil, *Phys. Med.* **61**, 18–27 (2019).
<https://doi.org/10.1016/j.ejmp.2019.04.004>
18. Quality Assurance for Computed Tomography—Diagnostic and Therapy Applications. https://www-pub.iaea.org/MTCD/Publications/PDF/Pub1557_web.pdf. Accessed June 5, 2021.
19. K. P. Chang, T. K. Hsu, W. T. Lin, and W. L. Hsu, *Radiat. Phys. Chem.* **140**, 260–265 (2017).
<https://doi.org/10.1016/j.radphyschem.2017.02.006>
20. Radioprotection, Module of Quality Control and Radioprotection in Tomodensitometry (2013).
21. A. M. A. Roa and H. K. Andersen, *J. Appl. Clin. Med. Phys.* **16**, 350–365 (2015).
<https://doi.org/10.1120/jacmp.v16i2.4972>
22. M. Rezaee and D. Letourneau, *J. Med. Imaging Radiat. Sci.* **50**, 297–307 (2019).
<https://doi.org/10.1016/j.jmir.2019.01.005>

23. PMMA Phantom for CT Performance with Convenience, Radcal Corporation **626**, 91016 (2015).
24. The Chamber for Computed Tomography Dose Index (CTDI), Another Industry Standard, Radcal Corporation, 4500054 (2011).
25. F. Zarb, . Rainford, and M. F. McEntee, Radiography **17**, 109–114 (2011).
<https://doi.org/10.1016/j.radi.2010.10.004>
26. K. Tang, L. Wang, R. Li, J. Lin, X. Zheng, and G. Cao, “Effect of low tube voltage on image quality, radiation dose, and low-contrast detectability at abdominal multidetector CTa: Phantom study,” J. Biomed. Biotechnol. **2012**, 130169 (2012).
<https://doi.org/10.1155/2012/130169>
27. C. Zaehring, A. Euler, G. M. Karwacki, et al., Clin. Radiol. **71**, 615.e1–615.e6 (2016).
<https://doi.org/10.1016/j.crad.2016.02.014>
28. M. Beeres, M. Romer, B. Bodelle, et al., Cancer Imaging **14**, 28 (2014).
<https://doi.org/10.1186/s40644-014-0028-7>